



STUDY ON VORTICAL STRUCTURE OF A TRANSVERSE JET USING CFD

Kanako Komuro¹ and Tetsuhiro Tsukiji²

ABSTRACT

Vortical structure formations caused by the interaction of a turbulent jet issuing transversely into a uniform stream are simulated with the aid of Fluent ver.6.3 CFD package. For preparing for the improvement of existing boundary layer control system using the transverse jet, this research focuses on calculating basic transverse jet flow field with a jet injected at 90° to the crossflow and seeking appropriate analytical method for this issue. Jet-to-crossflow velocity ratio is set to 4.0 which is realized as the wake structure is formed most orderly and corresponding wake Strouhal number (0.13) by Fric and Roshko (1994), and crossflow Reynolds number is set to 3800. The calculating zone contains 548,000 hexahedral cells and the large eddy simulation – LES is used for the viscous model. The results visualized by vorticity iso-surface and velocity vectors clearly describe the vortical structural of the wake. In particularly, the results show the intense counter-rotating vortex pair and wake vortices convected downstream. The effect of the wake on the wall is investigated by drawing distribution of wall shear stress which is compared with velocity profile near the wall. These results confirm that wake vortices contribute to decreasing shear stress especially downstream of the jet.

Keywords: Transverse jet, Vortex, Boundary layer control, Computational Fluid Dynamics

INTRODUCTION

Vortex generator which generates longitudinal vortex into the crossflow is commonly used as boundary layer control system. Transverse jet equipment is also well known as the active control system of the boundary layer, whose vortical structure is complex as shown in Fig. 1. Four types of coherent structure can be discerned in the near field of the jet, where the three-dimensional interaction between the jet and crossflow is most intense. In Fig. 1, they are the following: (1) the jet shear-layer vortices; (2) the system of horseshoe vortices; (3) the counter-rotating vortex pair; and (4) the wake vortices. These vortices are reported as very complicated and, particularly, the wake vortices have unique flow pattern, and fundamentally different from the well-known phenomenon of vortex shedding from solid bluff bodies by the experiments of the Fric and Roshko (1994). They conducted the series of experiments with the

¹ Graduate school of Science and Technology, Sophia University, Yotsuya Campus, 7-1. Kioi-cho, Chiyoda-ku, Tokyo 102-8554, e-mail: k-komuro@sophia.ac.jp

² Faculty of Science and Technology, Sophia University, Yotsuya Campus, 7-1. Kioi-cho, Chiyoda-ku, Tokyo 102-8554, e-mail: t-tukiji@sophia.ac.jp

help of flow visualization and hot-wire anemometry, and described the structural features of the wake downstream of the jet and investigated wake profile in details. To compare the present results with experimental flow pattern, important physical model parameters are corresponded to their experiment. A number of previous investigations addressed the wake behind the jet, but still the transverse jet remain to be simulated the complex wake structure and improved the boundary control system by analyzing with various parameters. Thus the purpose of the present calculation is to describe the vortical structure with simple transverse jet set-up, and confirm reliability for establishing analytical method for this problem. Also, the primary effect on a wall which is given by the wake vortices as wall shear stress is addressed in the present report.

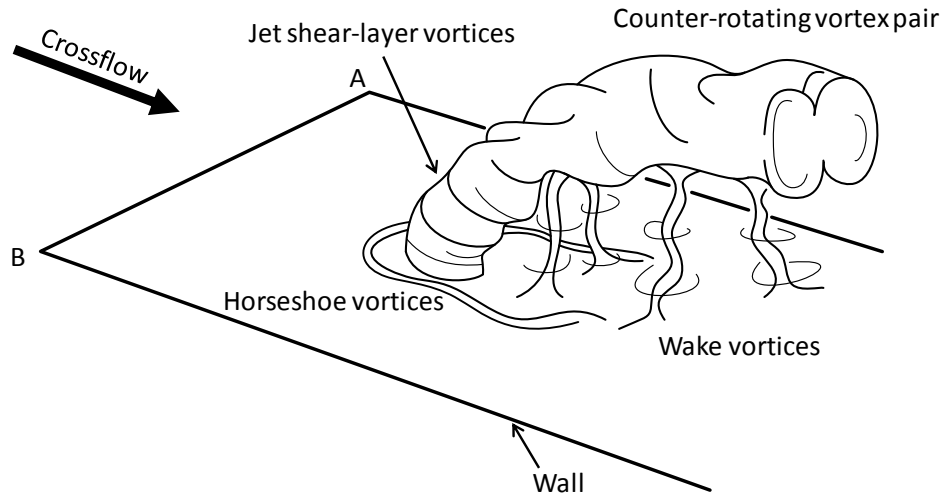


Fig. 1. Sketch of four types of vortical structure

FLOW SETUP AND ANALYTICAL METHOD

The important physical parameters of flow set-up depend on the experiment of Fric and Roshko (1994) with which the present results are compared are given in Table 1. Crossflow Reynolds number is defined as $U_{cf} D_j / \nu$, where U_{cf} , D_j and ν are nominal mean crossflow velocity, diameter of the jet orifice and kinematic viscosity of air, respectively. The most important physical model parameter defining the transverse jet is the jet to crossflow velocity ratio V_R . In this simulation, V_R is set to 4.0 which is reported to form most ordinary wake vortices downstream of the jet and define the wake Strouhal number (0.13) most sharply. Parameters such as calculating domain size, numerical model or time step are defined by comparisons of reliability with different parameter in this research. Dimensioned drawing with coordinate system of calculation zone is shown in Fig. 2. A single jet injected at 90° to the crossflow and the exit diameter D_j is set to 38mm to the wall in a flow domain of $20D_j \times 8D_j \times 10D_j$ in the x -streamwise, y -spanwise and z -stream-normal directions. Also, the part names are indicated in Fig. 2, for example, “plane-ABCD” represent the wall from which the jet issue. As given Table. 2, the boundary conditions for the problem are uniform inlet velocity at the crossflow inlet and the jet orifice, outflow at the outlet, no-slip at the wall, and slip at the top surface and both sides. The calculating zone consists of 548,000 hexahedral cells as shown in Fig. 3. This cell size is considered as limit for the efficient calculation when the present analytical method applied to the system with multiple jets. Analytical parameters are given in Table. 3. Solver is Fluent ver. 6.3 CFD package and the large eddy simulation – LES is used for the viscous model to analyze complicated unsteady flow field.

Table 1. Physical model parameters

| Parameter | Symbol | Value |
|---------------------------|-----------|---------|
| Crossflow Reynolds number | Re_{cf} | 3800 |
| Jet orifice diameter | D_j | 38 mm |
| Crossflow velocity | U_{cf} | 1.5 m/s |
| Velocity ratio | V_R | 4 |

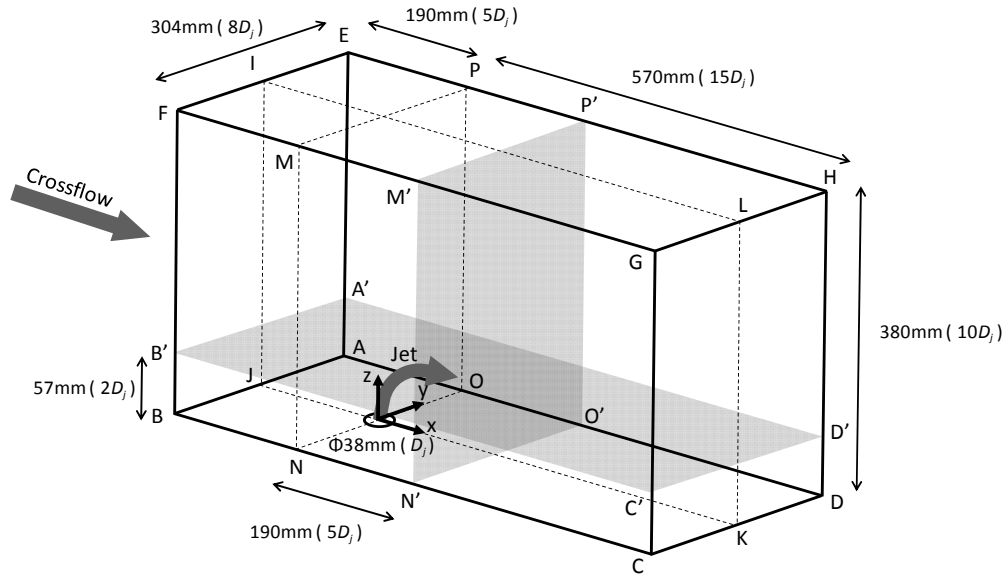


Fig. 2. Dimensioned drawing of calculation zone

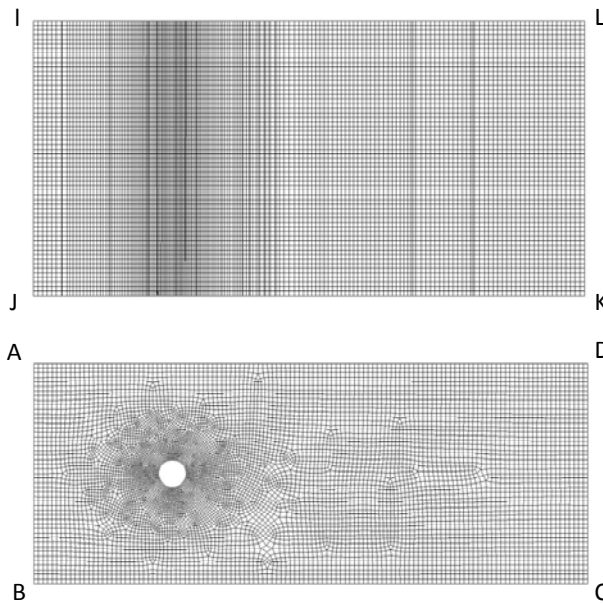


Fig. 3. Profile of meshes

Table 2. Boundary Conditions

| Zone | Type | Value |
|------------------------------|------------------------|---------|
| Computational domain | Fluid | Air |
| Crossflow inlet (plane-ABFE) | Uniform inlet velocity | 1.5 m/s |
| Jet orifice | Uniform inlet velocity | 6.0 m/s |
| Outlet (plane-CDHG) | Outflow | - |
| Plane wall (plane-ABCD) | Wall (no-slip) | 0 m/s |
| plane-BCGF, ADHE, EFGH | Symmetry (slip) | - |

Table 3. Analytical parameters

| Parameter | Value |
|----------------|-----------------------|
| Solver | Fluent ver.6.3 |
| Viscous model | Large Eddy Simulation |
| Cell size | 548,000 |
| Residuals | 0.0001 |
| Time step size | 0.0001 s |

RESULTS & DISCUSSION

To begin the results discussion with, the 3D view of visualized result is shown in Fig. 4 which give us good understanding of the wake vortices structure. There are the counter-rotating vortex pair and five wake vortices 0 to 4, around which the velocity vectors are described rotating flow. Note that scale of the vectors is fixed and the component of velocity vectors in the x -direction are defined by $U_x - U_{cf}$, i.e. observing from crossflow system. For the wake vortices are rotating, interaction of its structure provide low speed area on plane-A'B'C'D' as shown Fig.5. This is the important results that contribute to good effect on the wall -ABCD), which is discussed in the end of this session with the description of wall shear stress distribution.

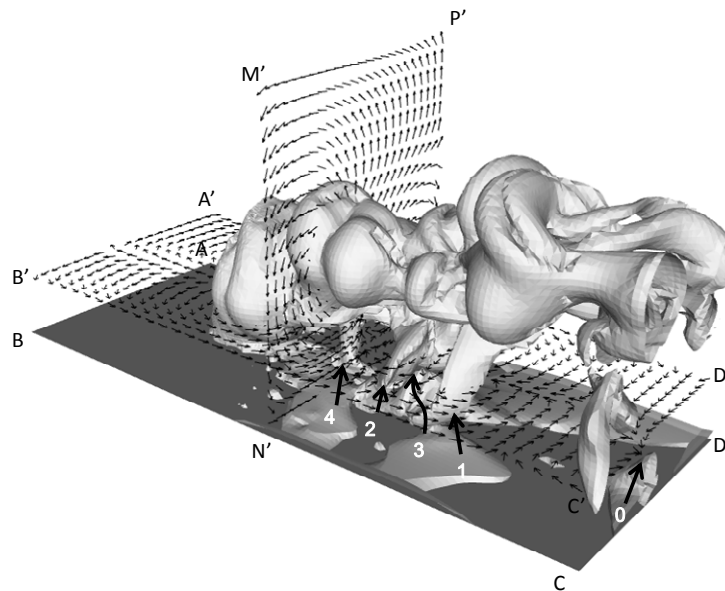


Fig 4. 3D diagram of vorticity iso-surface and velocity vectors

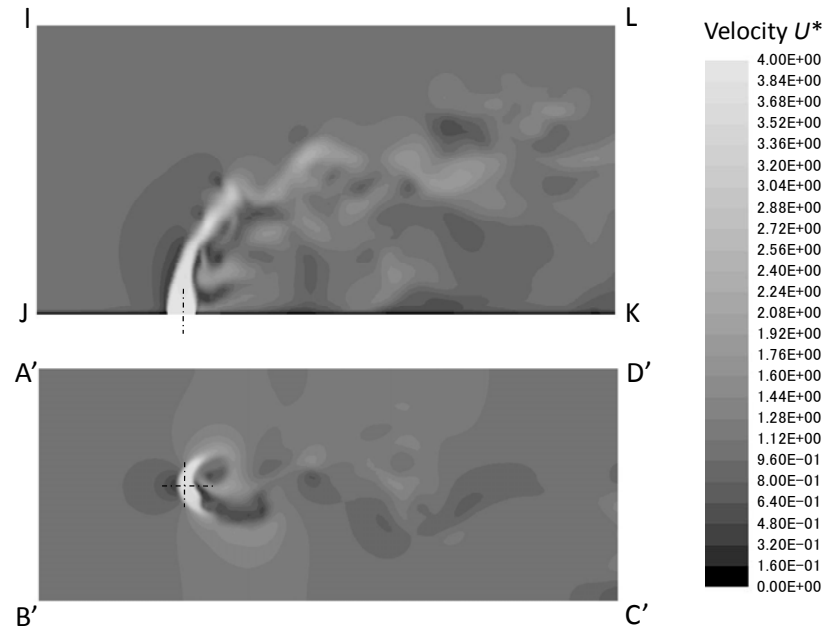


Fig. 5. Contours of velocity magnitude U^*

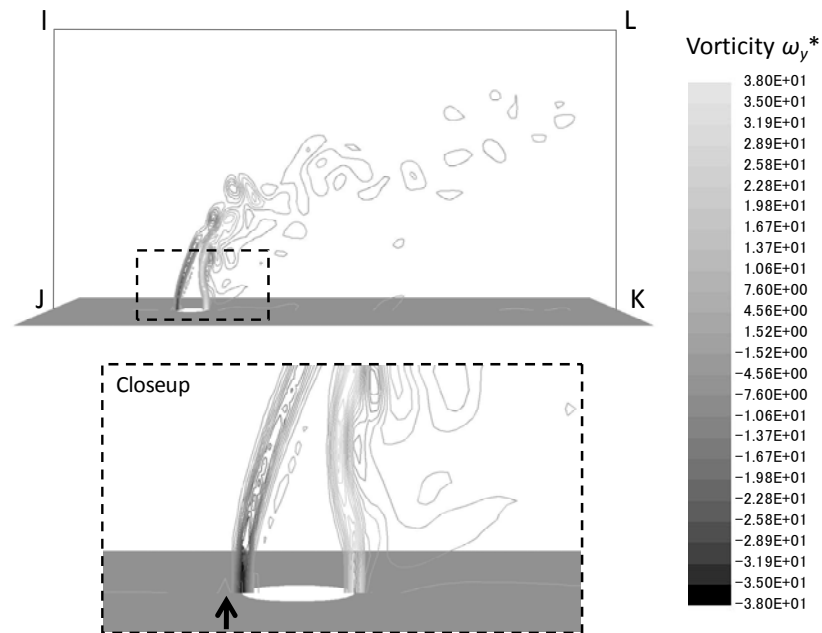


Fig. 6. Contours of vorticity ω_y^*

Vorticity in the y -direction $\omega_y^* = \omega_y D_j / U_{cf}$ on the plane-IJKL describe the jet shear-layer vortices as shown in Fig. 6. The jet shear-layer vortices dominate the initial portion of the jet, which are a result of the Kelvin-Helmholtz instability of the annular shear layer that separates from the edge of the jet orifice. Again, in Fig. 6, there is a short contour of vorticity pointed by the arrow in closeup view, where the horseshoe vortices are supposed to exist. The horseshoe vortices are so small that there is no clear

description of the horseshoe vortices by visualizing vorticity, except the single contour. More large size of cells may enable to simulate these minute vortices, but in this case, the primary purpose is to describe the major feature of the transverse jet and find out the good analytical method for improving the effect on the wall with appropriate cell size for efficient calculations.

Fig. 7 show that five images of the wake vortices at intervals of time = 0.08 s for analyzing convection of the wake vortices downstream of the jet. The first picture indicated in Fig. 7(a) is at the same time with the result shown in Fig. 4-6, 8 and 9. Side views of vorticity iso-surface are given in the left, and top views of velocity vectors on the plane-A'B'C'D' observed from crossflow system are in the right. The numbers presenting in these pictures mark the positions of the wake vortices. Some of them indicated as "(#)" are the number of invisible wake vortex in that figure, i.e. the wake vortices behind the other part of iso-surface or beneath the surface-A'B'C'D' of vectors. Some vectors without the wake vortex number which seem to describe the vortices are not wake vortex but the description of the portion of the counter-rotating vortex pair. It is corresponding to the experiment result that the flow around a transverse jet does not separate from the jet and does not shed vorticity into the wake. Instead, the wake vortices have their origins in the laminar boundary layer of the wall from which the jet issues (see the eruption of wake vortex-5 in Fig. 7(b)). These result in eruptions of boundary-layer fluid and formation of wake vortices that are convected downstream. In the present result of simulation, wake vortices are not always shed alternately like Karman-vortex wake, for example, the wake vortices 2-4 have same rotation direction. For that reasons, it is hard to account the cycle of the wake vortices and derive the wake Strouhal number to compare with experimental result of $St_w \approx 0.13$ measured by Fric and Roshko (1994).

$$St_w = \frac{f_w D_j}{U_{cf}} \quad (1)$$

The wake Strouhal number is defined by Eq. (1) above, $St_w \approx 0.13$ can be converted to the wake vortex cycle 0.19 s. At time = 0.32 s, the wake vortex-4 has already passed the point where the wake vortex-0 exist at time = 0 s, i.e. 2 cycle has passed. However the calculating result has 2.6 s in total time, the present St_w is derived nearly 0.127 by taking the average. This Strouhal number depends on wake vortex cycle when it given by every two vortices passing the point with neglecting the rotation direction. Again, the wake vortices are irregularly formed, not always have inverse rotation direction to next vortex, so that this St_w is not as clear as the result of the experiment.

Researching the effect of the wake on the wall is important to evaluate the transverse jet as boundary control system. Fig. 8 show that the wall shear stress in the x -direction $\tau_x^* = 2 \tau_x / \rho U_{cf}^2$ on plane-ABCD. To compare the shear stress distribution with the wake vortex structure, velocity vectors on the surface $Z/D_j = 0.2$ above the plane-ABCD are also indicated in Fig. 8. Again, note that the vectors are observed from crossflow system. It is obvious that the flow pattern of wake vortices provide the low shear stress area downstream of the jet. To see more in details, the comparisons of distribution of wall shear stress τ_x^* and velocity U_x^* on the line-JK are plotted in Fig. 9. Note that x -axis of the graph begin with $X/D_j = 0$ which is center of the jet orifice, NOT point-J, and U_x^* is the data on $Z/D_j = 0.2$ above the line-JK. As wall shear stress is defined in Eq. (2), where μ is viscosity of air, wall shear stress τ_x is proportional to the gradient of U_x . For this reason, it is confirm that the plotting of wall shear stress τ_x^* trace the velocity U_x^* changes.

$$\tau_x = \mu \frac{\partial U_x}{\partial z} \quad (2)$$

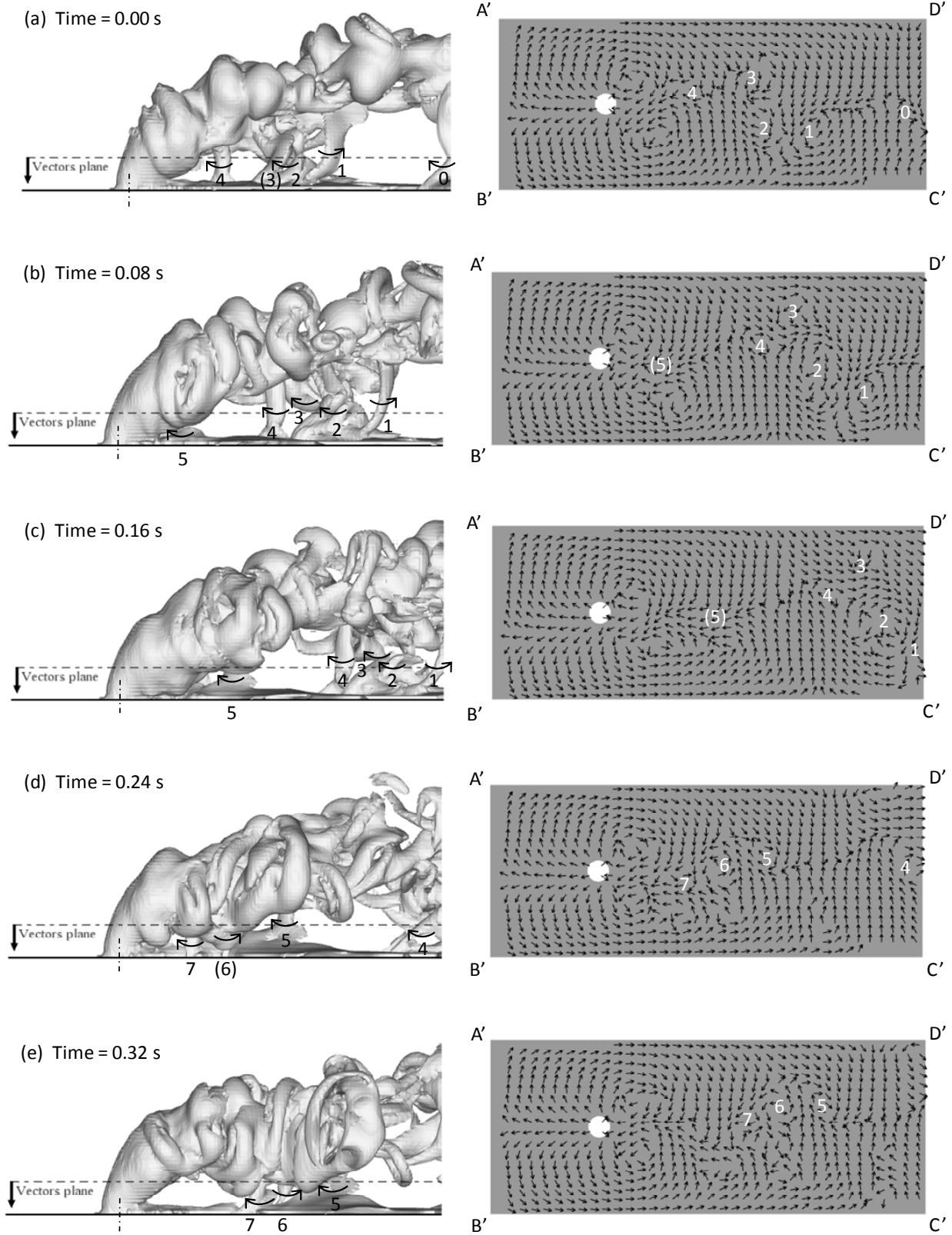


Fig. 7. Convection of the wake vortices

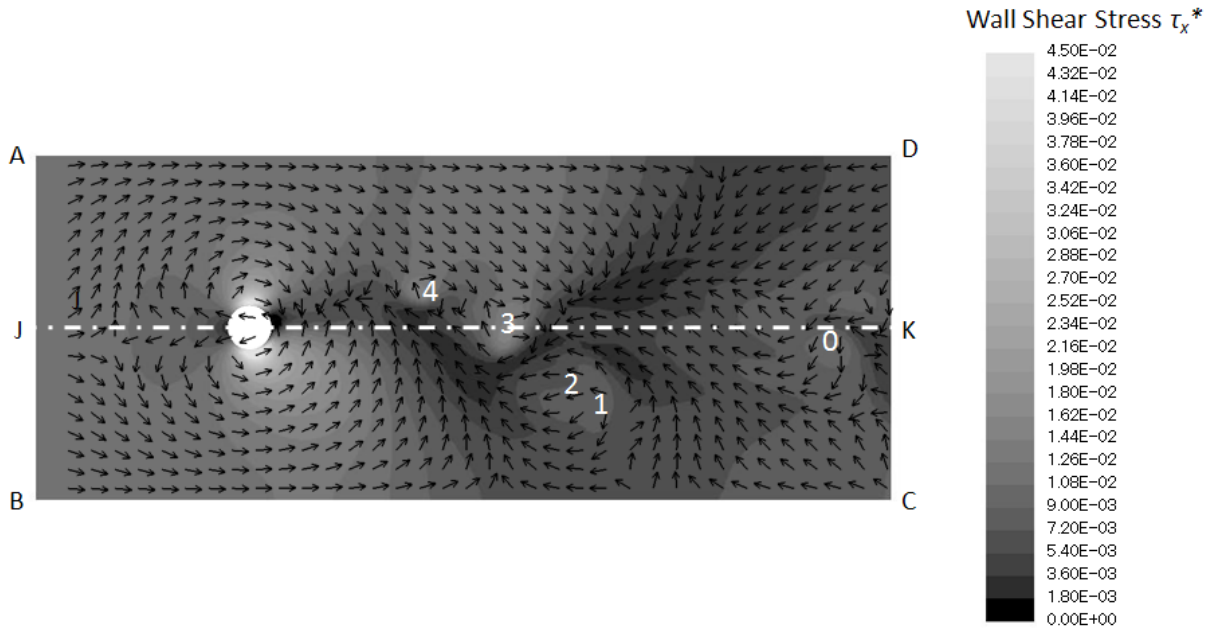


Fig. 8. Contours of wall shear stress τ_x^* ($Z/D_j=0$) and vectors of velocity ($Z/D_j=0.2$)

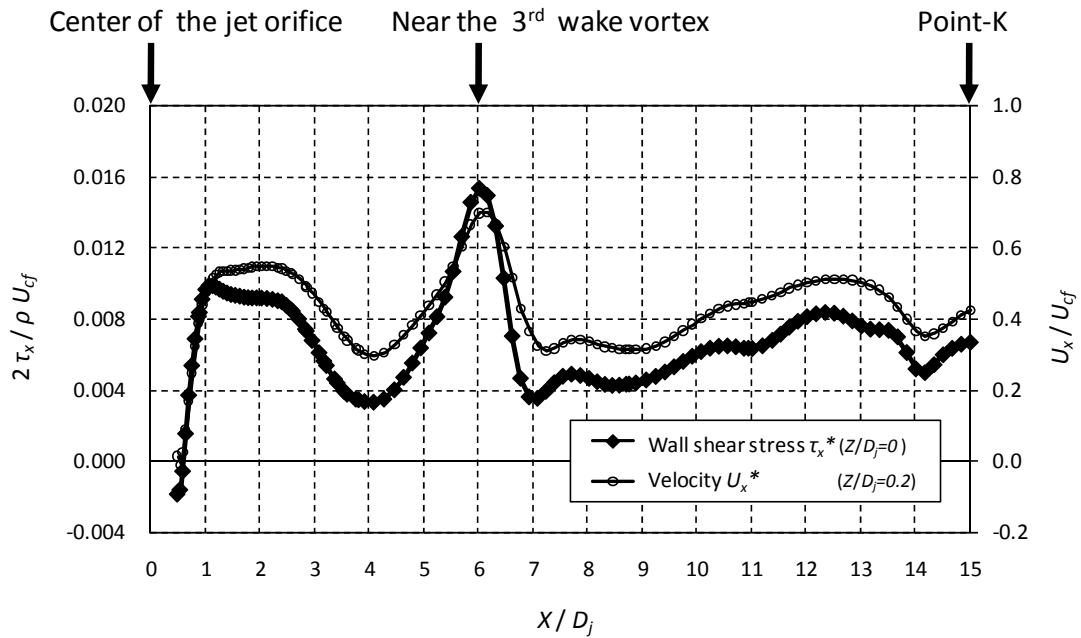


Fig. 9. Distribution of wall shear stress τ_x^* ($Z/D_j=0$) and velocity U_x^* ($Z/D_j=0.2$) on line-JK

SUMMARY AND CONCLUSIONS

With the aid of Fluent ver.6.3 CFD package, the complex flow field of transverse jet is simulated at the jet-to-crossflow velocity ratio 4.0. The present numerical method using LES realizes the description of the three-dimensional coherent vortices which is resulting from interaction of the jet and crossflow. Also the effect of the wake vortices on the wall is confirmed by the relation between the wall shear stress distribution and wake vortices locations. For these results, availability of the present analytical method is verified.

Here are conclusions derived by the present calculation results.

- The jet shear-layer vortices are described by the result of vorticity contours in the initial portion of the jet.
- Comparing with the observation of the experiment, the formation of the wake vortices is irregular but the wake Strouhal number 0.127 is corresponding to the measurement ($St_w \approx 0.13$) by Fric and Roshko (1994).
- The profile of the wake vortices provides the low speed region downstream of the jet, which contributes to decreasing shear stress on the wall.
- The intense counter-rotating vortex pair is described by visualizing the vorticity iso-surface, which may affect the separation point when the boundary layer control system is required in adverse gradient flow field.

REFERENCES

T. F. Fric and A. Roshko (1994), “Vortical structure in the wake of a transverse jet”, J. Fluid Mech., vol.279, pp. 1-47

APPENDIX I. NOTATION

The following symbols were used as superscript or subscript.

- * nondimensional parameter
- x physical component in the x -direction
- y physical component in the y -direction
- z physical component in the z -direction
- cf crossflow
- j jet
- w wake vortex